PHYSICAL REVIEW A **79**, 011605(R) (2009)

Bloch oscillations of a Bose-Einstein condensate in a subwavelength optical lattice

Tobias Salger,[1] Gunnar Ritt,[2,*] Carsten Geckeler,[1,2] Sebastian Kling,[1] and Martin Weitz[1]
[1]*Institut für Angewandte Physik, Universität Bonn, Wegelerstrasse 8, D-53115 Bonn, Germany*
[2]*Physikalisches Institut, Universität Tübingen, Auf der Morgenstelle 14, D-72076 Tübingen, Germany*
(Received 12 November 2007; published 21 January 2009)

We report on experiments studying the transport properties of an atomic Bose-Einstein condensate in an optical lattice of spatial period $\lambda/2n$, where n is an integer, realized with the dispersion of multiphoton Raman transitions. We observe Bloch oscillations, as a clear effect of quantum transport, in a subwavelength-scale periodicity lattice. An unusually large tunneling coupling between lattice sites is evident from the measured effective mass. Future prospects of the different lattice structures are expected in the search for new quantum phases in tailored lattice structures up to quantum computing in optical nanopotentials.

DOI: 10.1103/PhysRevA.79.011605 PACS number(s): 03.75.Lm, 37.10.−x, 42.50.Wk

Optical lattices have developed into successful model systems for effects known or predicted in solid-state physics [1]. Bloch oscillations, in which an atom subject to a force performs an oscillatory rather than a uniformly accelerated motion, are one of the most striking quantum transport properties arising from the periodic potential [2]. In other works, concepts such as number squeezing [3] or the Mott-insulator transition [4] were investigated. Further, Landau-Zener transitions have been studied in optical lattices of variable spatial symmetry [5]. So far, all experiments studying quantum transport and exploring the strongly correlated regime have been carried out in optical lattices with $\lambda/2$ or above spatial periodicity—i.e., with a periodicity that does not beat the Rayleigh resolution limit. Conventional optical lattices are formed by atoms confined in the antinodes of an optical standing wave by light forces that the $\lambda/2$ spatial periodicity of the trapping potential is naturally imprinted onto the atomic wave function.

Motivated by the quest to increase the resolution of optical microscopy as well as to write smaller lithographic features, multiphoton and entangled photon techniques have been investigated for the resolving of subwavelength spatial structures [6–8]. In general, both a nth-order multiphoton process and a process involving n entangled photons can lead to a n-fold increase in the spatial resolution. Other developments yielding an optical resolution beyond the Rayleigh limit include 4π and stimulated emission depletion (STED) microscopy [9]. Subwavelength-periodicity optical lattices are of interest also in the context of developing beam splitters for atom interferometers with large spatial separation between the paths [10–12].

Here we report on the observation of Bloch oscillations of atoms in lattices for which the lattice periodicity is clearly below the Rayleigh resolution limit. The small spatial periodicity of the investigated tightly bound subwavelength lattice leads to an increased Bloch period. Within our experimental uncertainties, no Bragg diffraction signal is observed when accelerating atoms in the subwavelength lattice to the first band edge of a conventional standing-wave lattice. The transport signals along with the determined effective mass in a $\lambda/4$-periodicity subwavelength lattice are compared to the results obtained with a conventional lattice of $\lambda/2$ spatial periodicity. Besides a modification in the Bloch period, we also find a striking difference in the effective atomic masses, which is ascribed to the large tunnel coupling between sites in the high-spatial-periodicity subwavelength lattice.

Let us begin by describing our scheme to create sub-Rayleigh-resolution optical lattices for cold atoms. The trapping potential of conventional lattices is determined by the ac-Stark shift in optical standing waves. In a quantum picture, the absorption of one photon of a running-wave mode followed by the stimulated emission of a photon into a counterpropagating mode contributes to the trapping potential. A lattice with spatial periodicity of a fractional harmonic $\lambda_{\mathrm{eff},n}/2=\lambda/2n$ could in principle be achieved by replacing each of the absorption and emission cycles with a stimulated multiphoton process induced by n photons, as indicated in Fig. 1(a). Here, $\lambda_{\mathrm{eff},n}$ denotes the effective wavelength of a n-photon field [13]. However, unwanted standing-wave effects with $\lambda/2$ spatial periodicity also appear in this process. Figure 1(b) shows the scheme used for a four- and a six-photon lattice with potential periodicities of $\lambda/4$ and $\lambda/6$, correspondingly [5,10,14,15]. Compared to the ladder scheme, in this improved method, absorption (stimulated emission) processes have been exchanged by stimulated emission (absorption) processes of an oppositely directed photon. The high resolution of Raman spectroscopy between two stable ground states over an excited state here allows us to clearly separate in frequency space the desired $2n$th-order process from lower-order contributions.

Our experimental setup has been described previously [14,16]. Briefly, a rubidium (^{87}Rb) Bose-Einstein condensate is produced all-optically by evaporative cooling in a quasistatic CO_2-laser dipole trap. During the final stages of the evaporation, a magnetic field gradient is activated, resulting in a spin-polarized condensate with roughly 10^4 atoms in the $m_F=-1$ Zeeman component of the $F=1$ hyperfine ground state. The lattice beams are generated by splitting the emitted beam of a tapered diode laser into two and directing each of the partial beams through an acousto-optic modulator. The modulators are used for beam switching and also to superimpose different optical frequency components onto a single

*Present address: FGAN-FOM, Gutleuthausstraße 1, D-76275 Ettlingen, Germany.

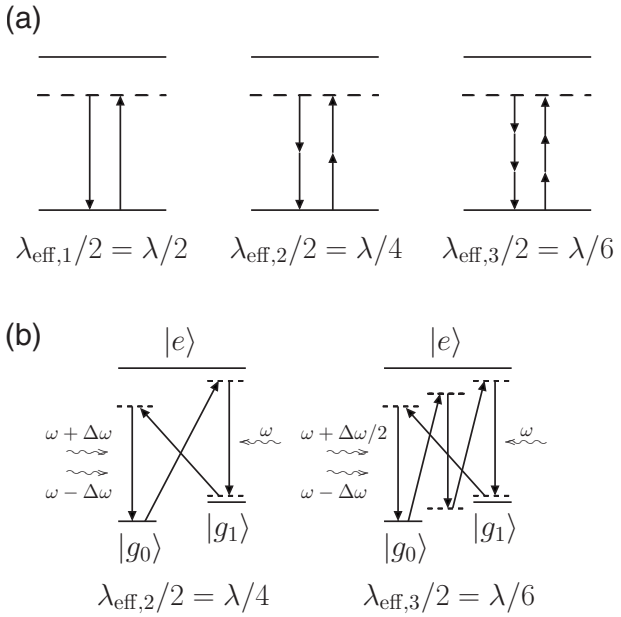

FIG. 1. Scheme for the generation of lattice potentials with higher spatial periodicities. (a) Left: second-order processes in a usual standing-wave lattice, yielding a spatial periodicity of $\lambda/2$ of the trapping potential. Middle and right: four-photon (six-photon) processes contributing to a $\lambda/4$ ($\lambda/6$) spatial periodicity lattice potential. However, in these simple schemes the usual standing-wave potential induced by two-photon processes dominates. (b) Improved scheme for the generation of a four-photon (left) and six-photon (right) lattice potential, as used in this work. In contrast to the schemes indicated in (a), two-photon standing-wave processes are here suppressed.

beam path, as required for the generation of the multiphoton potentials with the schemes shown in Fig. 1(b). The beams are sent through optical fibers and focused in a counterpropagating geometry onto the Bose-Einstein condensate. Respectively to the horizontally oriented CO_2-laser dipole trapping beam, the lattice beams are inclined under an angle of 41°. For the realization of multiphoton lattices shown in Fig. 1(b), we use the $F=1$ ground-state Zeeman components $m_F=-1$ and 0 as levels $|g_0\rangle$ and $|g_1\rangle$ and the $5P_{3/2}$ manifold as the excited state $|e\rangle$. A magnetic bias field of 1.8 G removes the degeneracy of the Zeeman components. For a measurement of Bloch oscillations, the lattice beams are initially ramped up with a linear ramp within 20 μs to adiabatically load the atoms into the lowest band of the lattice potential. This procedure was applied for the usual two-photon as well as for the multiphoton lattice potentials. One of the lattice beams was subsequently acousto-optically detuned with a constant chirp rate [for the four-photon lattice scheme shown on the left-hand side of Fig. 1(b), a single beam with frequency ω was used] to accelerate the lattice, respectively, to the atomic rest frame. After a variable acceleration time, the lattice beams were extinguished and the atomic momentum distribution was recorded with a time-of-flight absorption imaging technique.

To verify the effective creation of a subwavelength optical lattice, we have studied far-field diffraction of atoms off the lattice potentials. The atoms here were exposed to the periodic potentials imprinted by 6-μs-long optical pulses of the lattice beams. Figure 2 shows corresponding atomic time-of-flight images recorded after a 12-ms-long free expansion time and reconstructed lattice potentials for (a) a conventional lattice, (b) a four-photon lattice, and (c) a six-photon lattice. For the higher-order multiphoton lattices, the spacing between diffraction orders is increased due to the smaller spacing between sites of the corresponding periodic potential. For sufficiently short pulses and small pulse areas, the time-of-flight images are closely connected to the reciprocal lattice, but also for more general pulses an analysis of such images allows for a determination of lattice parameters [13]. The spirit of these preparatory experiments much resembles atom diffraction and interferometry work with high-momentum transfer of Refs. [17–19].

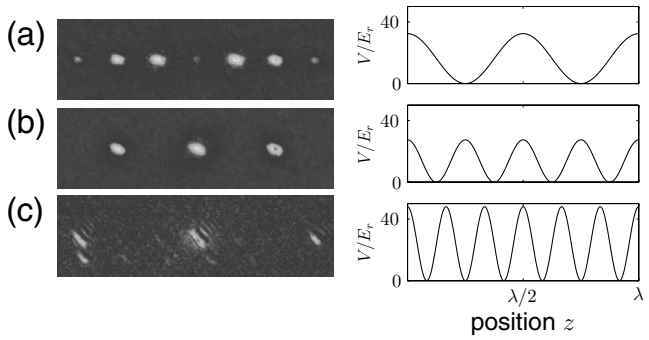

FIG. 2. The figures on the left-hand side show far-field diffraction images of a rubidium-Bose-Einstein condensate off (a) a usual standing-wave lattice with $\lambda/2$ spatial periodicity, (b) a four-photon multiphoton lattice with $\lambda/4$ periodicity, and (c) a six-photon lattice with $\lambda/6$ periodicity. A Stern-Gerlach magnetic field was applied in an angle of 45° relatively to the horizontal axis, which allows for a resolution of the atomic Zeeman structure. The figures on the right-hand side show the corresponding reconstructed lattice potentials.

Quantum transport of cold atoms in optical lattices much resembles the behavior of electrons in crystal lattices [20]. In a one-dimensional atom potential of the form $V(x) = V_0 \cos^2(\pi x/d)$, where $d=\lambda/2n$ denotes the lattice periodicity with n as an integer number and V_0 the lattice depth, the energy spectrum splits up into bands. They can be labeled by the eigenenergies $E_j(q)$ of the eigenstates $|j,q\rangle$, where j denotes the band index and q the atomic quasimomentum, and $E_j(q)$ and $|j,q\rangle$ are periodic functions of the quasimomentum q with period $2\pi/d=4\pi n/\lambda$. Conventionally, the quasimomentum q is restricted to the first Brillouin zone: i.e., $|q| \leqslant \hbar\pi/d=n\hbar k$. Thus, the first Brillouin zone of a $2n$th-order multiphoton lattice with spatial periodicity $\lambda/2n$ spans a n-fold larger quasimomentum range than a conventional standing-wave lattice of periodicity $\lambda/2$. At the first band gap, states with quasimomentum $q \in \{-n\hbar k, n\hbar k\}$ are coupled due to Bragg reflection, which leads to an energy splitting between the lowest and first excited bands, and similar couplings also occur between higher bands. When an external force F is applied, the quasimomentum evolves in time and is determined by $q(t)=q(0)+Ft$. At the band gaps we expect, the wave packets are Bragg reflected, if the force is weak enough, not to cause Landau-Zener transitions to higher bands, so that the evolution is periodic in time, where

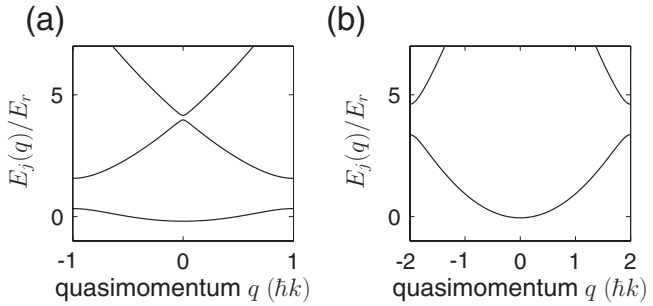

FIG. 3. Band structure for atoms in a periodic lattice potential of (a) $\lambda/2$ and (b) $\lambda/4$ spatial periodicity, respectively. The used lattice depth was $2.7E_r$ in both cases.

$T_B = n\hbar k/F$ denotes the period, required for the wave packet to evolve over the full Brillouin zone. The atomic group velocity $\langle v\rangle = dE(q(t))/dq$ here oscillates with time. The expected band structure for our lattice potentials is shown in Fig. 3 for a two- and a four-photon lattice, respectively.

Experimentally we have adjusted the depth of the lattice potentials for both lattices to be around $2.7E_r$ (with $E_r = \hbar^2k^2/2m$ corresponding to the photon recoil energy), as was monitored by Rabi oscillations [21]. For a measurement of Bloch oscillations, the atomic Bose-Einstein condensate is adiabatically loaded into the lowest band of the lattice potentials at zero quasimomentum ($q=0$). Subsequently, the lattice potential is accelerated respectively to the atomic rest frame by applying a linear variation of one of the Raman beam frequencies. In this way, a constant inertial force $F=-ma$ is exerted onto the atoms, where m is the atomic mass of the rubidium atoms and $a \approx 6.4\ \mathrm{m/s^2}$. The experimental setup is basically the same, as was described in detail in [5]. Figure 4 shows the mean atomic velocity relatively to the lattice as a function of acceleration time t_a for both two- and four-photon lattice potentials. For small acceleration times, the atomic velocity increases linearly with time, as predicted by Newton's second law for a free atom. We expect that an

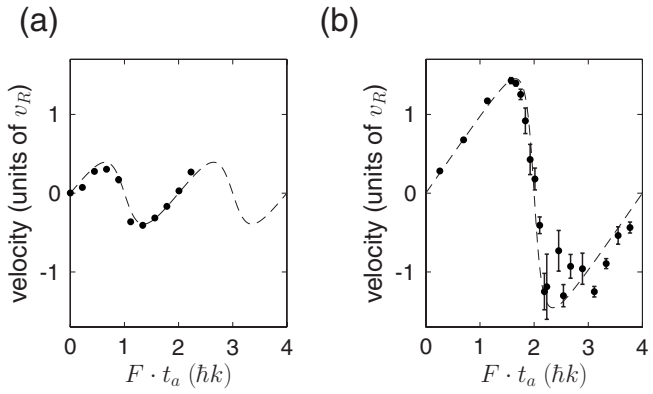

FIG. 4. Mean atomic velocity as a function of the acceleration time t_a for (a) a usual optical lattice and (b) a four-photon lattice with $\lambda/4$ spatial periodicity. For the data points with no visible error bar, the estimated uncertainty is below the drawing size of the dots. The dashed line shows a fit to the data based on a theoretical model, where the Landau-Zener tunneling rate to the next higher Bloch band ($\approx 10\% - 15\%$, respectively) was the only free fit parameter.

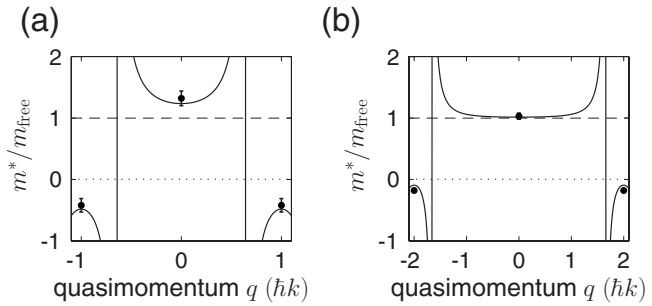

FIG. 5. Effective mass of atoms in the lowest Bloch band as a function of quasimomentum for (a) a usual standing-wave lattice with $\lambda/2$ spatial periodicity and (b) a four-photon lattice with $\lambda/4$ spatial periodicity. The dots with error bars are experimental points, derived from the derivative of the (interpolated) Bloch oscillation data of Fig. 4 for the shown specific values of q. The solid lines show the result of a theoretical calculation.

acceleration continues until the edge of the first Brillouin zone, which is reached at a quasimomentum $q=\hbar\pi/d$, where $d=\lambda/2n$ denotes the spacing from site to site. With $n=1$ and 2 for two- and four-photon lattices, the band edge occurs at $q=\hbar k$ and $2\hbar k$, respectively, as shown in Fig. 3. For the conventional two-photon lattice, we as in earlier work [2] observe that the wave packet is Bragg reflected near $Ft_a \approx \hbar k$. On the other hand, for the $\lambda/4$-spatial-periodicity four-photon lattice the atoms are accelerated until $Ft_a \approx 2\hbar k$ is reached. In both cases Bragg reflection occurs at the corresponding band gap. The atomic wave packets are reflected to the corresponding negative-momentum value and full Bloch oscillations are observed. The demonstration of this phenomenon for a $\lambda/4$-periodicity multiphoton lattice directly shows the coherence of atom transport in such sub-Rayleigh-periodicity structures. The Bloch period T_B in the smaller-periodicity four-photon lattice is a factor of 2 longer than that of the conventional lattice. A more detailed comparison of the shapes of the observed oscillations in Fig. 4, both of which were recorded for comparable lattice depths, shows that the slope steepness near the band edge is larger in the multiphoton lattice than that of the standing-wave potential. Furthermore, the atomic acceleration near zero momentum is very similar to that of a free atom for the microscopic $\lambda/4$-periodicity lattice, while a somewhat larger difference is observed for the conventional lattice. These effects can be described in terms of the effective masses m^*. The atomic dynamics can be described using the usual equation of motion, $F=m^*d\langle v\rangle/dt$, when accounting for an effective mass $m^*(q)=2/(d^2E/dq^2)$, which in general differs from the mass of a free atom due to the periodic potential. From our experimental data, we have determined the effective atomic masses both at $q=0$ and obtained $m^*=(1.29\pm0.12)m_{free}$ and $m^*=(1.03\pm0.05)m_{free}$ for the two- and four-photon lattices, respectively, and at the band edge at $q=n\hbar k$, which yields $m^*=(-0.42\pm0.11)m_{free}$ and $m^*=(-0.18\pm0.02)m_{free}$ for two- and four-photon lattices, respectively. Figure 5 shows these data points for the effective atomic mass overlayed with the theoretical prediction (solid lines) as a function of quasimomentum for both lattices. It turns out that, for the smaller-periodicity four-photon lattice, the effective mass

near $q=0$ is much closer to the real atomic mass than in the usual $\lambda/2$-periodicity lattice, which can be understood in terms of the larger distance from the band edge for the multiphoton lattice. If we compare the tunneling matrix element $J(n)$, defined in the Bose-Hubbard model [22], in the high-periodicity lattice with the tunneling rate $J(1)$ in the case of an optical standing wave of the same potential depth, we get the following relation:

$$\frac{J(n)}{J(1)} \propto \sqrt{n}\exp(-a/n), \tag{1}$$

where n is an integer and a is a constant number. This formula is strictly valid in the limit $V_0 \gg n^2 E_r$, where V_0 denotes the lattice depth and E_r the recoil energy, but for the experimentally used parameters still gives an approximate scaling. One clearly sees the enhancement of the tunneling matrix element when reducing the distance $d=\lambda/2n$ between neighboring lattice sites. A further interesting issue of our multiphoton lattice is that the ground-state wave-function size decreases with the small spatial periodicity. We expect that the effects of interatomic on-site interactions are enhanced.

To conclude, we have observed Bloch oscillations of atoms in a different, sub-Rayleigh-periodicity optical lattice. Evidence for a comparatively large tunneling coupling between sites in the short-periodicity lattice is obtained from the measured effective atomic mass. We expect that the observed effects can have applications in the development of nanoscale quantum computing schemes and the modeling of solid-state physics problems. Note that a reaching of, e.g., the Mott-insulator transition in short-periodicity lattices is favored by larger tunneling rates and stronger interatomic interactions with a decreased spacing from site to site. An alternative perspective includes the Fourier synthesis of arbitrarily shaped lattice structures with quantum gases realized by superimposing lattices of different spatial periodicities, which allows for a dynamic tailoring of solid-state-like structures. It would be also of great interest to investigate how nonlinear effects, caused by the interaction between atoms in a Bose-Einstein condensate, are influenced in such a sub-Rayleigh optical-lattice potential. One could, for instance, compare the lifetime of Bloch oscillations in lattices with different spatial periodicities.

We acknowledge financial support from the Deutsche Forschungsgemeinschaft and the Landesstiftung Baden-Württemberg.

[1] See, e.g., I. Bloch, Nat. Phys. **1**, 23 (2005).
[2] M. Ben Dahan, E. Peik, J. Reichel, Y. Castin, and C. Salomon, Phys. Rev. Lett. **76**, 4508 (1996).
[3] C. Orzel, A. K. Tuchman, M. L. Fenselau, M. Yasuda, and M. A. Kasevich, Science **291**, 2386 (2001).
[4] M. Greiner, O. Mandel, T. Esslinger, T. W. Hänsch, and I. Bloch, Nature (London) **415**, 39 (2002).
[5] T. Salger, C. Geckeler, S. Kling, and M. Weitz, Phys. Rev. Lett. **99**, 190405 (2007).
[6] E. Yablonovitch and R. B. Vrijen, Opt. Eng. **38**, 334 (1999).
[7] A. N. Boto, P. Kok, D. S. Abrams, S. L. Braunstein, C. P. Williams, and J. P. Dowling, Phys. Rev. Lett. **85**, 2733 (2000).
[8] S. Bentley and R. Boyd, Opt. Express **12**, 5735 (2004).
[9] M. Dyba and S. W. Hell, Phys. Rev. Lett. **88**, 163901 (2002).
[10] P. R. Berman, B. Dubetsky, and J. L. Cohen, Phys. Rev. A **58**, 4801 (1998).
[11] M. Weitz, T. Heupel, and T. W. Hänsch, Phys. Rev. Lett. **77**, 2356 (1996).
[12] J. M. McGuirk, M. J. Snadden, and M. A. Kasevich, Phys. Rev. Lett. **85**, 4498 (2000).
[13] J. Jacobson, G. Bjork, I. Chuang, and Y. Yamamoto, Phys. Rev. Lett. **74**, 4835 (1995).
[14] G. Ritt, C. Geckeler, T. Salger, G. Cennini, and M. Weitz, Phys. Rev. A **74**, 063622 (2006).
[15] M. Weitz, G. Cennini, G. Ritt, and C. Geckeler, Phys. Rev. A **70**, 043414 (2004).
[16] G. Cennini, G. Ritt, C. Geckeler, and M. Weitz, Phys. Rev. Lett. **91**, 240408 (2003).
[17] P. E. Moskowitz, P. L. Gould, S. R. Atlas, and D. E. Pritchard, Phys. Rev. Lett. **51**, 370 (1983).
[18] D. M. Giltner, R. W. McGowan, and S. A. Lee, Phys. Rev. Lett. **75**, 2638 (1995).
[19] M. Kozuma *et al.*, Phys. Rev. Lett. **82**, 871 (1999).
[20] N. W. Ashcroft and N. D. Mermin, *Solid State Physics* (Saunders College Publishing, New York, 1976).
[21] O. Morsch, J. H. Müller, M. Cristiani, D. Ciampini, and E. Arimondo, Phys. Rev. Lett. **87**, 140402 (2001).
[22] W. Zwerger, J. Opt. B: Quantum Semiclassical Opt. **5**, S9 (2003).